



OPEN

# Cystathionine- $\gamma$ -lyase contributes to tamoxifen resistance, and the compound I194496 alleviates this effect by inhibiting the PPAR $\gamma$ /ACSL1/STAT3 signalling pathway in oestrogen receptor-positive breast cancer

Han Fu, Xue Han, Wenqing Guo, Xuening Zhao, Chunxue Yu, Wei Zhao, Shasha Feng, Jian Wang, Zhenshuai Zhang, Kaijian Lei<sup>✉</sup>, Ming Li<sup>✉</sup> & Tianxiao Wang<sup>✉</sup>

Tamoxifen (TAM) resistance is a major challenge in treating oestrogen receptor-positive (ER+) breast cancers. It is possible that the H<sub>2</sub>S synthase cystathionine- $\gamma$ -lyase (CSE), which has been previously shown to promote tumour growth and metastasis in other cancer cells, is involved in this resistance. Therefore, we investigated CSE's role and potential mechanisms in TAM-resistant breast cancer cells. First, we examined the effect of CSE expression on TAM sensitivity and resistance in MCF7 (breast cancer) cells. The findings revealed that CSE was directly associated with TAM sensitivity and involved in TAM resistance in ER+ breast cancer cells, indicating that it may be useful as a biomarker. Next, we wanted to determine the molecular mechanism of CSE's role in TAM resistance. Using cell migration, co-immunoprecipitation, western blotting, and cell viability assays, we determined that the CSE/H<sub>2</sub>S system can affect the expression of PPAR $\gamma$  by promoting the sulfhydrylation of PPAR $\gamma$ , which regulates the transcriptional activity of ACSL1. ACSL1, in turn, influences STAT3 activation by affecting the phosphorylation, palmitoylation and dimerization of STAT3, ultimately leading to the development of TAM resistance in breast cancer. Finally, we examined the effect of CSE inhibitors on reducing drug resistance to determine whether CSE may be used as a biomarker of TAM resistance. We observed that the novel CSE inhibitor I194496 can reverse TAM resistance in TAM-resistant breast cancer via targeting the PPAR $\gamma$ /ACSL1/STAT3 signalling pathway. Overall, our data indicate that CSE may serve as a biomarker of TAM resistance and that the CSE inhibitor I194496 is a promising candidate for combating TAM resistance.

**Keywords** Cystathionine- $\gamma$ -lyase (CSE), TAM, Resistance, CSE inhibitor, Breast cancer

Breast cancer is a substantial health concern for women<sup>1,2</sup>. Breast cancer is divided into four subtypes according to the mRNA levels of ER, progesterone receptor (PgR), and human epidermal growth factor receptor 2 (HER2)<sup>3,4</sup>. ER+ breast cancer is the most commonly diagnosed subtype, accounting for approximately 75% of all breast cancer cases<sup>5</sup>. For breast cancer patients with ER+ tumours, TAM is the first-line endocrine treatment. However, a considerable number of breast cancer patients develop resistance to TAM. Primary resistance affects 40–50% of patients, whereas secondary resistance affects 30–40%, posing a considerable hurdle to effective cancer treatment. As a result, understanding resistance mechanisms is critical for creating targeted medicines that reduce resistance.

The development of drug resistance in tumours is strongly associated with the occurrence of metastasis. Patients who are resistant to TAM may develop tumour metastasis, which can worsen their resistance to TAM.

School of Pharmacy, Henan University, North Part of Jinming Road, Kaifeng 475004, Henan, People's Republic of China. ✉email: leikaijian@126.com; liming96001@126.com; wtx1975@henu.edu.cn

Hydrogen sulfide (H<sub>2</sub>S), the third gas transmitter after nitric oxide (NO) and carbon monoxide (CO), may contribute to cancer metastasis<sup>6,7</sup>. Cystathionine-γ-lyase (CSE), an endogenous H<sub>2</sub>S synthase, is highly expressed in different cancers and has been found to increase cancer cell proliferation and metastasis in various studies<sup>8–12</sup>. These findings imply that CSE may serve as a potential therapeutic target to overcome TAM resistance in breast cancer. A variety of cancers show abnormal activation of signal transducer and activator of transcription 3 (STAT3)<sup>12,13</sup>. STAT3 has been shown to play a substantial role in the promotion of treatment resistance in breast cancer patients. The sustained activation of STAT3, which includes phosphorylation, palmitoylation, acetylation, and nitrosylation, is a critical characteristic of drug resistance in breast cancer<sup>14–17</sup>. Our previous research revealed a regulatory loop between CSE and STAT3 in breast cancer<sup>18,19</sup>. As a result, the CSE/H<sub>2</sub>S system could contribute to controlling TAM resistance in breast cancer through STAT3 signalling.

Long-chain acyl-CoA synthase 1 (ACSL1) expression has been shown to be abnormally enhanced in TAM-resistant breast cancer cells<sup>20</sup>, and the fatty acids activated by ACSL1 can directly activate STAT3 by increasing STAT3 palmitoylation<sup>21</sup>. As a result, ACSL1 may mediate the regulatory effect of CSE on STAT3. Peroxisome proliferator-activated receptor gamma (PPARγ) is a transcription factor that modulates the expression of ACSL1. When activated, PPARγ can increase ACSL1 transcription by binding to PPRE, a PPAR-responsive element located in the ACSL1 promoter region<sup>22,23</sup>. CSE may promote TAM resistance in breast cancer by influencing the ACSL1/STAT3 pathway via PPARγ. Further research is required to investigate the impact of CSE inhibitors on reducing drug resistance and to determine whether CSE may be used as a biomarker of TAM resistance.

In this study, we found that the CSE/H<sub>2</sub>S system was strongly related to TAM sensitivity in ER+ breast cancer cells and that high CSE expression was associated with TAM resistance in TAM-resistant breast cancer cells. The ACSL1/STAT3 pathway promoted TAM resistance, and CSE affected PPARγ binding to the ACSL1 promoter by interacting with it and promoting PPARγ sulfhydrylation in TAM-resistant breast cancer cells. I194496, a new CSE inhibitor, successfully affected TAM resistance through the PPARγ/ACSL1/STAT3 pathway. Finally, these data suggest a novel and successful strategy for managing breast cancer patients who have developed resistance to TAM.

Additionally, we discovered that CSE affected PPARγ binding to the ACSL1 promoter by interacting with PPARγ and promoting the sulfhydrylation of PPARγ in TAM-resistant breast cancer cells. These findings indicate that the ACSL1/STAT3 pathway supports the induction of TAM resistance by CSE.

## Results

### The CSE/H<sub>2</sub>S system is closely related to TAM sensitivity in ER-positive breast cancer cells

We initially explored the connection between CSE protein expression and TAM sensitivity in MCF7 and T47D cells. Western blot and MTS results revealed that MCF7 cells were less susceptible to high CSE expression than were T47D cells with low CSE expression (Fig. 1A–C). This finding demonstrated that CSE expression levels were negatively linked with TAM sensitivity in ER+ breast cancer cells. Moreover, we discovered that TAM elevated CSE expression and H<sub>2</sub>S levels in MCF7 and T47D cells in a time- and dose-dependent manner (Fig. 1D–K), suggesting that TAM affects the CSE/H<sub>2</sub>S system in ER+ breast cancer cells.

To further investigate the relationship between CSE and TAM sensitivity in ER+ breast cancer cells, we first used MCF7/CSE shRNA cells with downregulated CSE expression (Fig. 2A) and determined the effects of TAM on growth, proliferation, migration, invasion, and apoptosis. The results showed that TAM inhibited growth, proliferation, migration and invasion and promoted apoptosis in MCF7/shRNA cells more than in MCF7/Vector cells (Fig. 2B–K). These data suggested that decreasing CSE expression improved TAM sensitivity in ER+ breast cancer cells. Then, we performed experiments on T47D/CSE cells with upregulated CSE expression (Fig. 3A,B) to determine how TAM affects the growth, proliferation, migration, and invasion of T47D/CSE cells. TAM inhibited growth, proliferation, migration, and invasion considerably less in T47D/CSE cells than in T47D/vector cells (Fig. 3C–J). These data suggested that increasing CSE expression decreased TAM sensitivity in ER+ breast cancer cells.

All the above results indicate that the CSE/H<sub>2</sub>S system is closely related to TAM sensitivity in ER+ breast cancer cells.

### High expression of CSE is involved in TAM resistance in TAM-resistant breast cancer cells

To investigate the effect of CSE on TAM resistance in ER+ breast cancer, we constructed MCF7/TAM cells, which are TAM-resistant MCF7 cells with 2× resistance (Fig. 4A,B). We discovered that the CSE expression level in MCF7/TAM cells was significantly greater than that in sensitive MCF7 cells (Fig. 4C,D). Further research revealed that downregulating CSE dramatically increased the inhibitory effects of TAM on growth, proliferation, migration, and invasion and promoted apoptosis in MCF7/TAM cells (Fig. 4E–L). These results imply that increased CSE expression may contribute to TAM resistance in ER+ breast cancer cells.

### CSE promotes TAM resistance through the ACSL1/STAT3 pathway in TAM-resistant breast cancer cells

One of the key genes for TAM resistance is STAT3, and studies have shown that TAM-resistant MCF7 (MCF7/TAM) cells have increased levels of STAT3 tyrosine phosphorylation at position 705<sup>15</sup>. Furthermore, we previously discovered that CSE might regulate STAT3 expression and activity in MCF7 cells<sup>18</sup>. Thus, we investigated how CSE affects STAT3 protein expression and activity in MCF7/TAM cells. The findings demonstrated that the downregulation of CSE decreased STAT3 levels (Fig. 5C), suggesting that CSE could promote TAM resistance in ER+ breast cancer through STAT3. However, it is unclear how CSE modulates STAT3. The fatty acid transporter protein ACSL1 has been found to exhibit aberrantly elevated expression in TAM-resistant breast cancer<sup>20</sup>. Furthermore, investigations have revealed that ACSL1 can activate STAT3 by increasing its palmitoylation<sup>21</sup>.

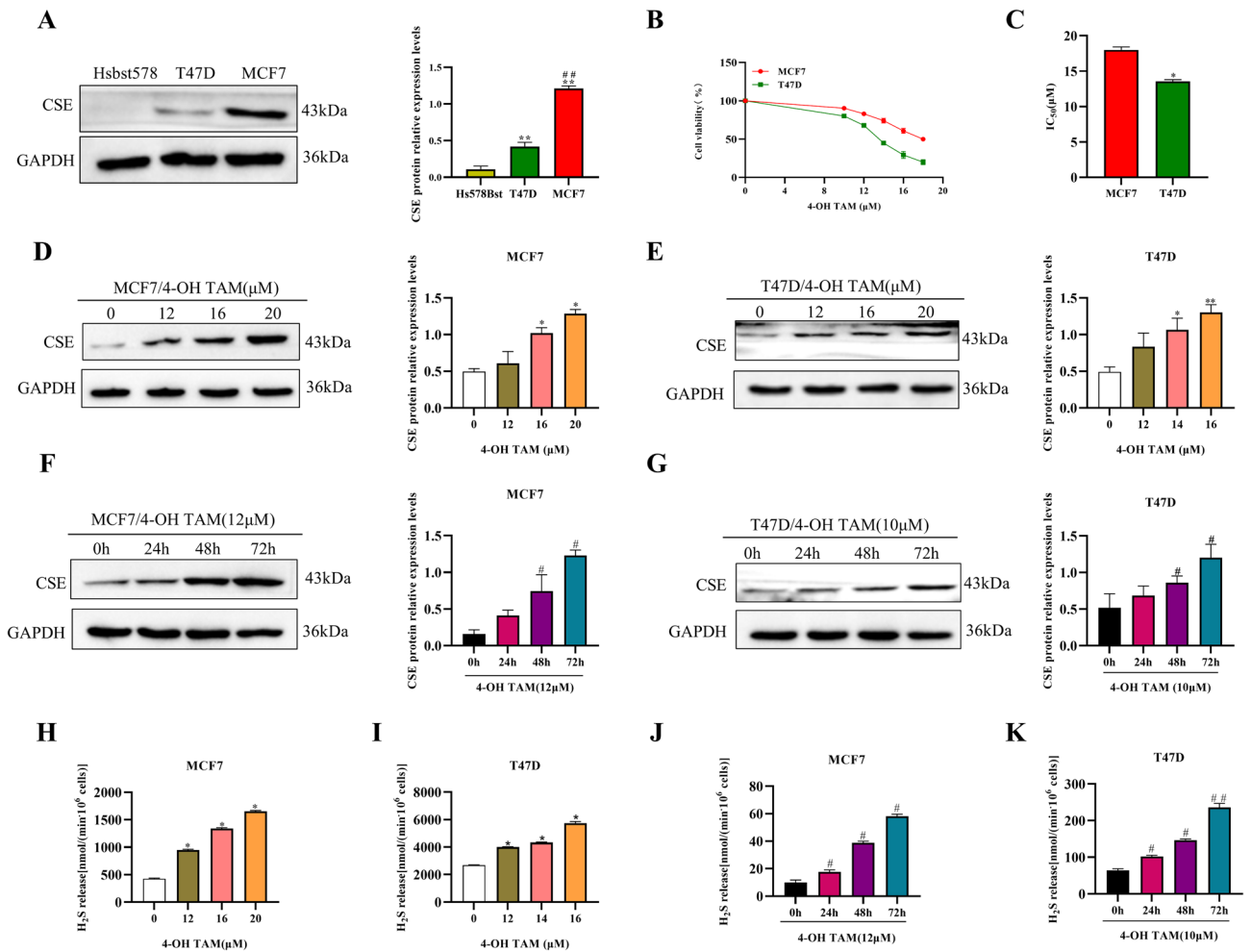


**Fig. 1.** CSE is highly expressed in ER+ breast cancer cells and negatively correlates with TAM sensitivity. **A** Expression levels of CSE proteins in two types of ER+ breast cancer cells and normal breast cells. MCF7 and T47D are ER+ breast cancer cell lines. Hsbst578 is a normal breast cell line. All data are expressed as mean  $\pm$  standard deviation ( $n = 3$ ).  $^{**}P < 0.01$  versus Hsbst578 cells;  $^{\#}P < 0.01$  versus T47D cells. **(B and C)** MTS method was used to detect the sensitivity and IC<sub>50</sub> value of MCF7 and T47D cells to 4-OH TAM. All data are expressed as mean  $\pm$  standard deviation ( $n = 3$ ).  $^{*}P < 0.05$  versus MCF7 cells. **(D–G)** The Western blot assay was used to detect the expression levels of CSE proteins in MCF7 and T47D cells as the duration and concentration of 4-OH TAM action increased. All data are expressed as mean  $\pm$  standard deviation ( $n = 3$ ).  $^{*}P < 0.05$ ,  $^{**}P < 0.01$  versus 0  $\mu\text{M}$  4-OH TAM group;  $^{\#}P < 0.05$ ,  $^{\#\#}P < 0.01$  versus 0 h group. **(H–K)** The methylene blue method was used to detect the level of H<sub>2</sub>S in MCF7 and T47D cells as the duration and concentration of 4-OH TAM action increased. All data are expressed as mean  $\pm$  standard deviation ( $n = 3$ ).  $^{*}P < 0.05$  versus 0  $\mu\text{M}$  4-OH TAM group;  $^{\#}P < 0.05$  versus 0 h group.

Thus, we investigated whether CSE modulates STAT3 via ACSL1. According to the Western blot results, ACSL1 and CSE were positively associated, and in MCF7/TAM cells, downregulating CSE inhibited the protein expression of ACSL1, STAT3, and pSTAT3 (Fig. 5A–D). Additionally, we discovered that in MCF7/TAM cells, CSE siRNA inhibited the palmitoylation of STAT3 (Fig. 5E–F). Furthermore, we found that in MCF7/TAM cells, the downregulation of ACSL1 dramatically decreased the expression of STAT3 and pSTAT3 and suppressed the palmitoylation of STAT3 (Fig. 5G–J). The above results suggest that in MCF7/TAM cells, ACSL1 mediates the regulatory impact of CSE on STAT3.

### CSE regulates ACSL1 expression by interacting with PPAR $\gamma$ and promoting the sulfhydrylation of PPAR $\gamma$ in TAM-resistant breast cancer cells

Research has demonstrated that the transcription factor PPAR $\gamma$  can bind to the ACSL1 promoter to modulate the expression of ACSL1<sup>22,23</sup>. Here, we investigated the relationship between CSE and PPAR $\gamma$  protein expression as well as the impact of CSE on the binding of PPAR to the promoter of ACSL1 to determine the mechanism by which CSE regulates ACSL1 in TAM-resistant breast cancer cells. The results demonstrated that in MCF7/TAM cells, the expression of PPAR $\gamma$  was positively correlated with that of CSE (Fig. 5B, 6A) and that the downregulation of CSE decreased the amount of the PPAR $\gamma$  protein (Fig. 6C,D). Moreover, the results of the luciferase assay demonstrated that the PPAR $\gamma$  binding activity to the ACSL1 promoter was markedly reduced in MCF7/TAM cells

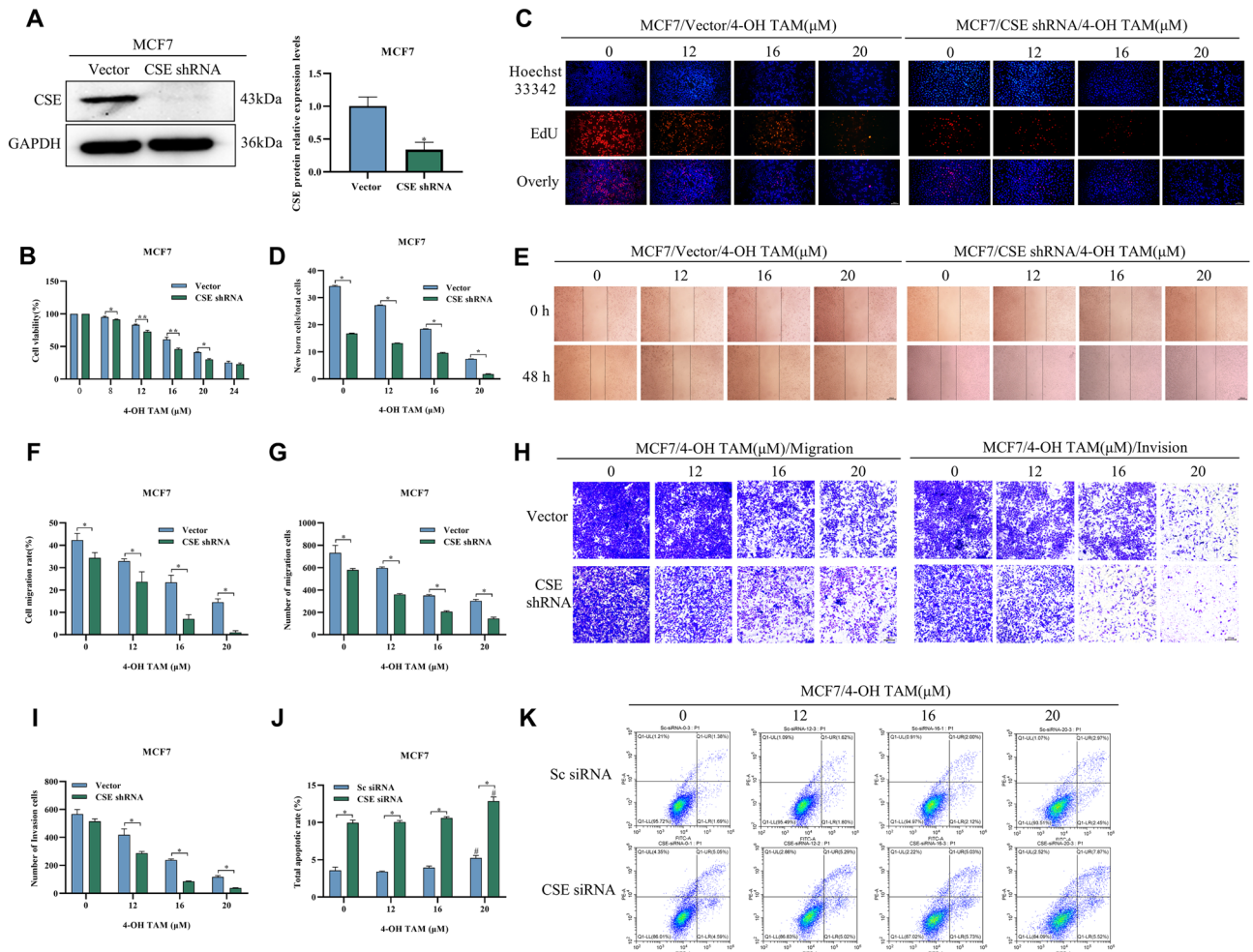


**Fig. 2.** Knocking down the expression of CSE in MCF7 cells can increase the inhibitory effect of TAM on the growth, proliferation, migration and invasion and the apoptosis-promoting effect of breast cancer cells. **(A)** Analysis of the efficiency of knocking down CSE proteins in MCF7 cells. **(B–D)** MTS and EdU assays were used to detect the effect of 4-OH TAM on the growth and proliferation of MCF7 cells after CSE knockdown. Representative images were taken. Scale bars, 100  $\mu$ m. **(E and F)** Wound healing assay was used to detect the effect of 4-OH TAM on the migration of MCF7 cells after CSE knockdown. Representative images were taken. Scale bars, 500  $\mu$ m **(G–I)** Transwell assay was used to determine the effect of 4-OH TAM on the migration and invasion of MCF7 cells after knockdown CSE expression. Representative images were taken. Scale bars, 200  $\mu$ m **(J and K)** Apoptosis assay was used to detect the effect of 4-OH TAM on apoptosis of MCF7 cells after knockdown of CSE expression. All data are expressed as mean  $\pm$  standard deviation ( $n = 3$ ). \* $P < 0.05$ , \*\* $P < 0.01$  versus the Vector group.

treated with CSE siRNA (Fig. 6F). Based on these data, it can be concluded that CSE regulates the ability of PPAR $\gamma$  to bind to the ACSL1 promoter in TAM-resistant breast cancer cells, hence affecting the expression of ACSL1.

Next, we investigated how CSE impacts PPAR $\gamma$ . A co-IP assay was used to determine the interaction between CSE and PPAR $\gamma$ . The results showed that CSE interacted with PPAR $\gamma$  in MCF7/TAM cells and that downregulating CSE expression greatly reduced this interaction (Fig. 6E). In addition, sulfhydrylation is a new type of protein posttranslational modification mediated by H $_2$ S. This process converts the sulfhydryl group of cysteine (-SH) to a persulfuryl group (-SSH) within the target protein, resulting in changes in protein activity or subcellular localization. This modification has recently sparked interest in the realm of biochemistry, offering a potential new avenue for understanding cellular signalling and regulation<sup>24</sup>. Therefore, we used a maleimide assay to detect the sulfhydrylation of PPAR $\gamma$ , providing valuable insight into the regulation of this vital protein. To calculate the PPAR $\gamma$  sulfhydrylation level, the decrease in green fluorescence intensity following DTT treatment was divided by the average total level of PPAR $\gamma$ <sup>25</sup>. The results showed that suppressing CSE decreased PPAR $\gamma$  sulfhydrylation in MCF7/TAM cells (Fig. 6G, H), indicating that CSE affects PPAR $\gamma$  activity through sulfhydrylation. The above data indicate that CSE interacts with PPAR $\gamma$  and promotes the sulfhydrylation of PPAR $\gamma$  to regulate PPAR $\gamma$  binding to the ACSL1 promoter, thus affecting the ACSL1/STAT3 pathway in TAM-resistant breast cancer cells.

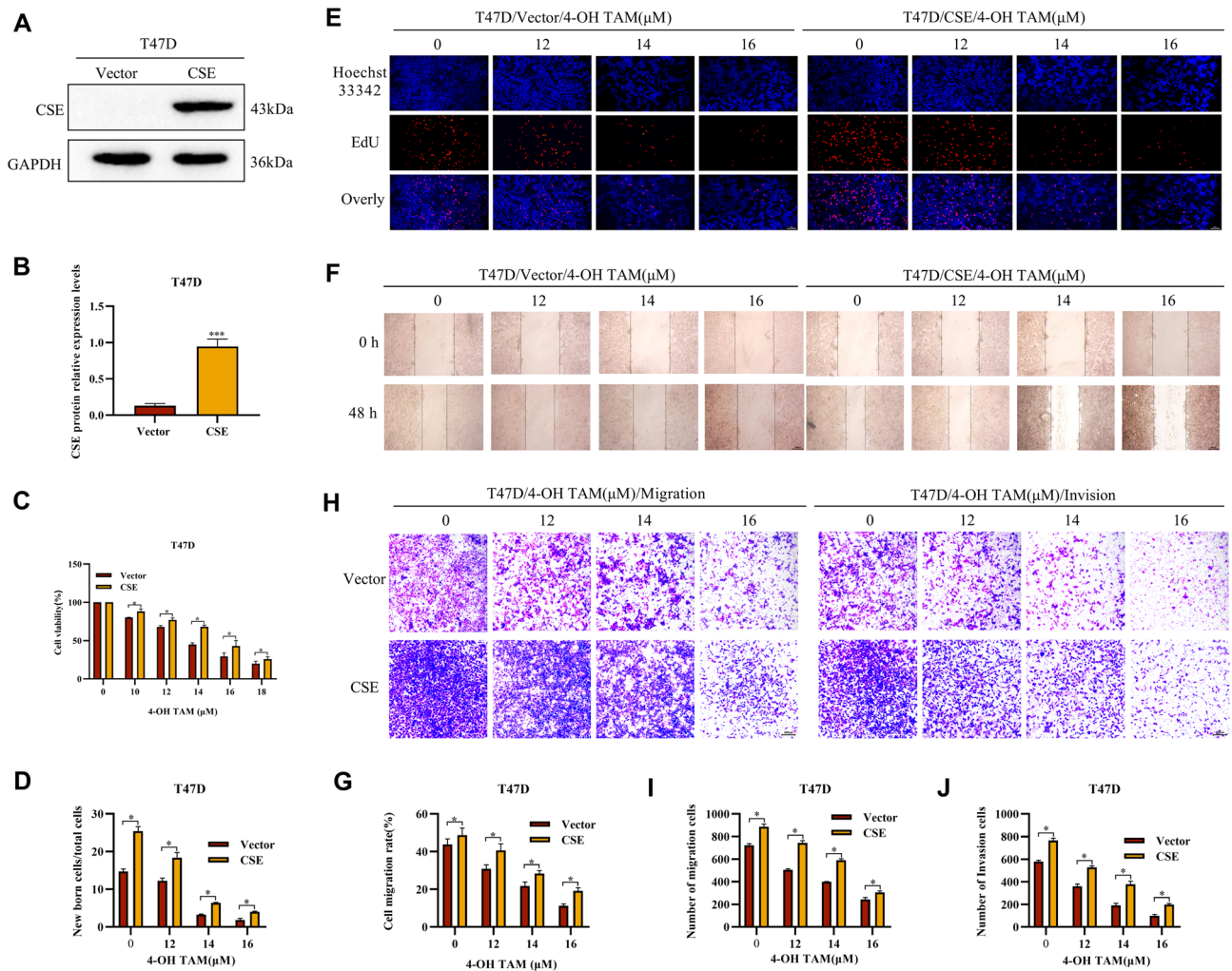


**Fig. 3.** Overexpression of CSE protein in T47D cells can increase the inhibitory effect of TAM on the growth, proliferation, migration and invasion of breast cancer cells. **(A and B)** Analysis of the efficiency of overexpression of CSE proteins in T47D cells. **(C–E)** MTS and EdU assays were used to detect the effect of 4-OH TAM on the growth and proliferation of T47D cells after upregulation of CSE, respectively. Representative images were taken. Scale bars, 100  $\mu\text{m}$ . **(F and G)** Wound healing assay was used to detect the effect of 4-OH TAM on the migration of T47D cells after upregulation of CSE. Representative images were taken. Scale bars, 500  $\mu\text{m}$ . **(H–J)** Transwell assay was used to determine the effect of 4-OH TAM on the migration and invasion of T47D cells after upregulation of CSE. Representative images were taken. Scale bars, 200  $\mu\text{m}$ . All data are expressed as mean  $\pm$  standard deviation ( $n = 3$ ). \* $P < 0.05$ , \*\*\* $P < 0.001$  versus the Vector group.

### I194496, a novel inhibitor of CSE, improves the sensitivity of TAM-resistant breast cancer cells to TAM treatment

These results suggest that increased expression of CSE in breast cancer promotes resistance to TAM. Consequently, the development of TAM resistance may be severely hampered by the targeted inhibition of CSE. A new CSE inhibitor called I194496 was found by virtual screening and confirmed through experimental methods<sup>19,26</sup>. Here, we investigated how I194496 affects the development of TAM resistance in MCF7/TAM and T47D/CSE cells. Compared with TAM alone, I194496 greatly enhanced the inhibition of cell growth, proliferation, migration, and invasion as well as the stimulation of cell death when combined with TAM (Fig. 7, 8). The results showed that I194496 significantly increased the inhibitory effect of TAM on cell growth, proliferation, migration, and invasion as well as its ability to enhance apoptosis induction, suggesting that TAM-resistant breast cancer cells are more susceptible to TAM therapy when a new CSE inhibitor is employed.

### I194496 alleviates TAM-induced resistance by inhibiting the PPAR $\gamma$ /ACSL1/STAT3 pathway

Building on previous research into the pathway by which CSE induces TAM resistance, we investigated the effect of I194496 on the PPAR/ACSL1/STAT3 pathway to better understand how I194496 counteracts TAM resistance. Western blot findings indicated that coadministration of I194496 and TAM significantly reduced PPAR $\gamma$ , ACSL1, and STAT3 protein levels in MCF7/TAM and T47D/CSE cells (Fig. 9A–D). Luciferase reporter gene assays showed that I194496 reduced PPAR $\gamma$  binding to the ACSL1 promoter and reversed the PPAR $\gamma$

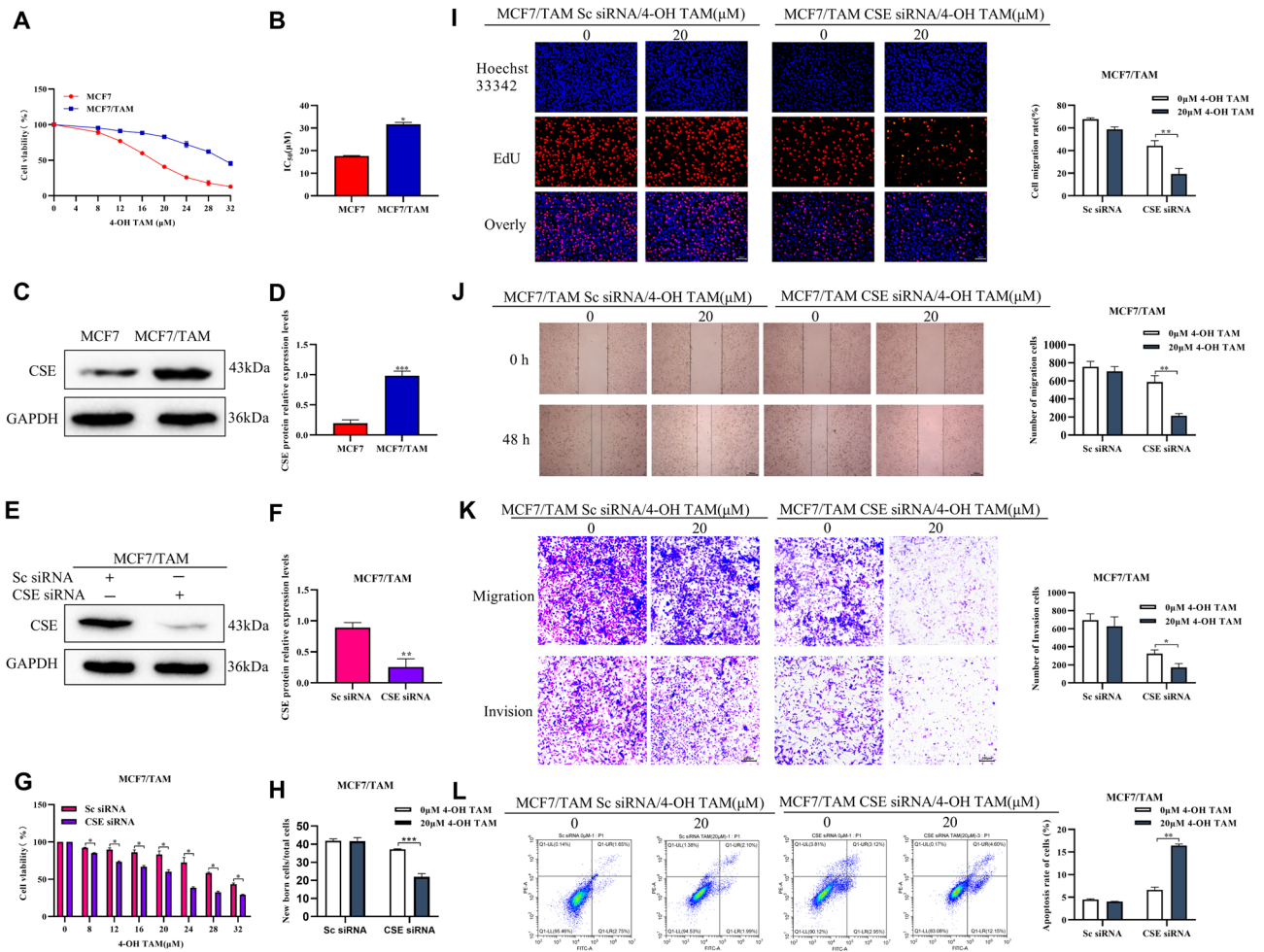


**Fig. 4.** Knocking down the expression of CSE in MCF7/TAM cells can increase the inhibitory effect of TAM on the growth, proliferation, migration and invasion and the apoptosis-promoting effect of breast cancer cells. (A and B) The MTS method was performed to detect the sensitivity and  $IC_{50}$  of MCF7 and MCF7/TAM cells to 4-OH TAM. All data are expressed as mean  $\pm$  standard deviation ( $n = 3$ ).  $^*P < 0.05$  versus MCF7 cells. (C and D) The expression levels of CSE proteins in MCF7 and MCF7/TAM cells. All data are expressed as mean  $\pm$  standard deviation ( $n = 3$ ).  $^{***}P < 0.001$  versus MCF7 cells. (E and F) Analysis of the efficiency of knocking down CSE proteins in MCF7/TAM cells. All data are expressed as mean  $\pm$  standard deviation ( $n = 3$ ).  $^*P < 0.05$  versus the Sc siRNA. (G–I) MTS and EdU assays were used to detect the effect of 4-OH TAM on the growth and proliferation of MCF7/TAM cells after CSE knockdown, respectively. Representative images were taken. Scale bars, 100  $\mu$ m. (J) Wound healing assay was used to detect the effect of 4-OH TAM on the migration of MCF7/TAM cells after CSE knockdown. Representative images were taken. Scale bars, 500  $\mu$ m. (K) Transwell assay was used to determine the effect of 4-OH TAM on the migration and invasion of MCF7/TAM cells after knockdown CSE expression. Representative images were taken. Scale bars, 200  $\mu$ m. (L) Apoptosis assay was used to detect the effect of 4-OH TAM on apoptosis of MCF7/TAM cells after knockdown of CSE expression. Representative images were taken. All data are expressed as mean  $\pm$  standard deviation ( $n = 3$ ).  $^*P < 0.05$ ,  $^{**}P < 0.01$  versus 0  $\mu$ M 4-OH TAM group.

binding to the ACSL1 promoter induced by TAM in MCF7/TAM and T47D/CSE cells (Fig. 9E,F). Additionally, an immunoprecipitation-acyl biotin replacement test was used to evaluate the effects of TAM, I194496, and the combination of both on STAT3 palmitoylation levels. The findings demonstrated that in T47D/CSE and MCF7/TAM cells, I194496 inhibited the palmitoylation of STAT3 and offset the effects of TAM on STAT3 palmitoylation (Fig. 9G–J). The results showed that I194496 employs the PPAR $\gamma$ /ACSL1/STAT3 pathway to overcome TAM resistance.

**Discussion**

TAM is currently the preferred endocrine therapy for ER+ breast cancer<sup>25</sup>. Nevertheless, patients with ER+ breast cancer may develop both primary and secondary TAM resistance<sup>27</sup>. Thus, understanding the mechanism of TAM resistance in ER+ breast cancer is critical for developing therapeutic options. This insight may eventually lead to better outcomes for patients with ER+ breast cancer.

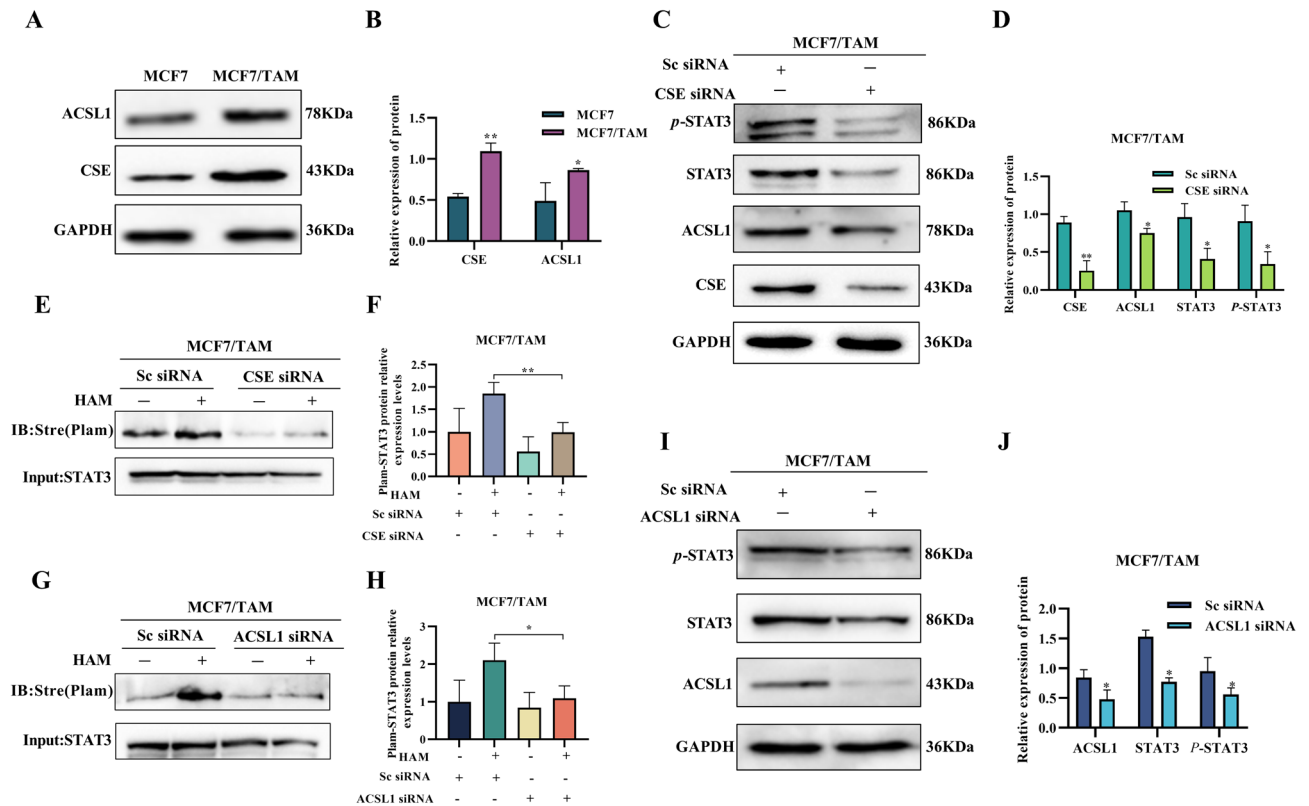


**Fig. 5.** CSE regulates the transcription of ACSL1 through PPAR $\gamma$  to affect the expression and activity of STAT3 protein, thereby participating in TAM resistance in ER+ breast cancer. **(A and B)** Expression levels of ACSL1 protein in MCF7/TAM resistant cells of ER+ breast cancer. All data are expressed as mean  $\pm$  standard deviation (n = 3). \* $P$  < 0.05 versus MCF7 cells group. \*\* $P$  < 0.01 versus MCF7 cells group. **(C and D)** The effect of down-regulation of CSE on the expression levels of ACSL1, STAT3 and p-STAT3 in MCF7/TAM cells. All data are expressed as mean  $\pm$  standard deviation (n = 3). \* $P$  < 0.05, \*\* $P$  < 0.01 versus Sc siRNA group. **(E and F)** The effect of downregulation of CSE protein on the palmitoylation level of STAT3 in MCF7/TAM cells. The acyl-biotin substitution method was applied to detect STAT3 palmitoylation. All data are expressed as mean  $\pm$  standard deviation (n = 3). \*\* $P$  < 0.01 versus Sc siRNA group. **(G and H)** Effect of down-regulation of ACSL1 protein on STAT3, p-STAT3 expression in MCF7/TAM. All data are expressed as mean  $\pm$  standard deviation (n = 3). \* $P$  < 0.05 versus Sc siRNA group. **(I and J)** Effect of down-regulation of ACSL1 protein on STAT3 palmitoylation in MCF7/TAM. All data are expressed as mean  $\pm$  standard deviation (n = 3). \* $P$  < 0.05 versus Sc siRNA group.

The CSE/H<sub>2</sub>S system has been shown to improve resilience to chemotherapy and endocrine therapy in breast cancer patients<sup>28</sup>. As a result, CSE may be a useful therapeutic target for reducing TAM resistance in breast cancer. This study revealed that the CSE/H<sub>2</sub>S system is connected to TAM sensitivity in ER+ breast cancer. The findings also revealed that high levels of the CSE/H<sub>2</sub>S system were the reason for TAM resistance in breast cancer patients. These discoveries could help improve therapeutic options for breast cancer patients.

STAT3 contributes significantly to treatment resistance in breast cancer patients. Strategies targeting fatty acid oxidation are being investigated as potential cancer therapies<sup>29</sup>. ACSL1 regulates both fatty acid production and oxidation pathways<sup>22</sup>. According to previous studies, oxidized fatty acids can increase STAT3 palmitoylation and directly activate this signalling pathway<sup>21</sup>. To elucidate the mechanism by which CSE promotes TAM resistance and make recommendations for overcoming this problem, we studied the effect of the CSE/H<sub>2</sub>S system on the ACSL1/STAT3 pathway. CSE was reported to promote TAM resistance in TAM-resistant breast cancer cells via the ACSL1/STAT3 pathway.

PPAR $\gamma$  is a transcription factor that modulates the expression of ACSL1. PPAR $\gamma$  can activate the transcription of the ACSL1 gene by binding to PPRE, the major PPAR response element in the ACSL1 promoter<sup>23</sup>. To determine whether the CSE/H<sub>2</sub>S pathway impacts ACSL1 transcription via PPAR $\gamma$ , we investigated the impact of CSE on the binding of PPAR $\gamma$  to the ACSL1 promoter. We found that the level of CSE affects the ability of PPAR $\gamma$  to bind to the ACSL1 promoter.

Co-IP was performed to study how CSE modulates PPAR $\gamma$  expression, which plays a role in TAM resistance in breast cancer. The results showed that CSE interacted with PPAR $\gamma$  in resistant breast cancer cells, and downregulation of CSE expression reduced this interaction. Furthermore, investigations have revealed that H<sub>2</sub>S can affect protein activity through sulfhydrylation<sup>24</sup>. We used a maleimide assay to detect the sulfhydrylation of PPAR $\gamma$ , providing insight into its regulation. These data suggested that CSE may modify the sulfhydrylation of PPAR $\gamma$ , potentially affecting its activity. These findings emphasize the necessity of studying the mechanisms by

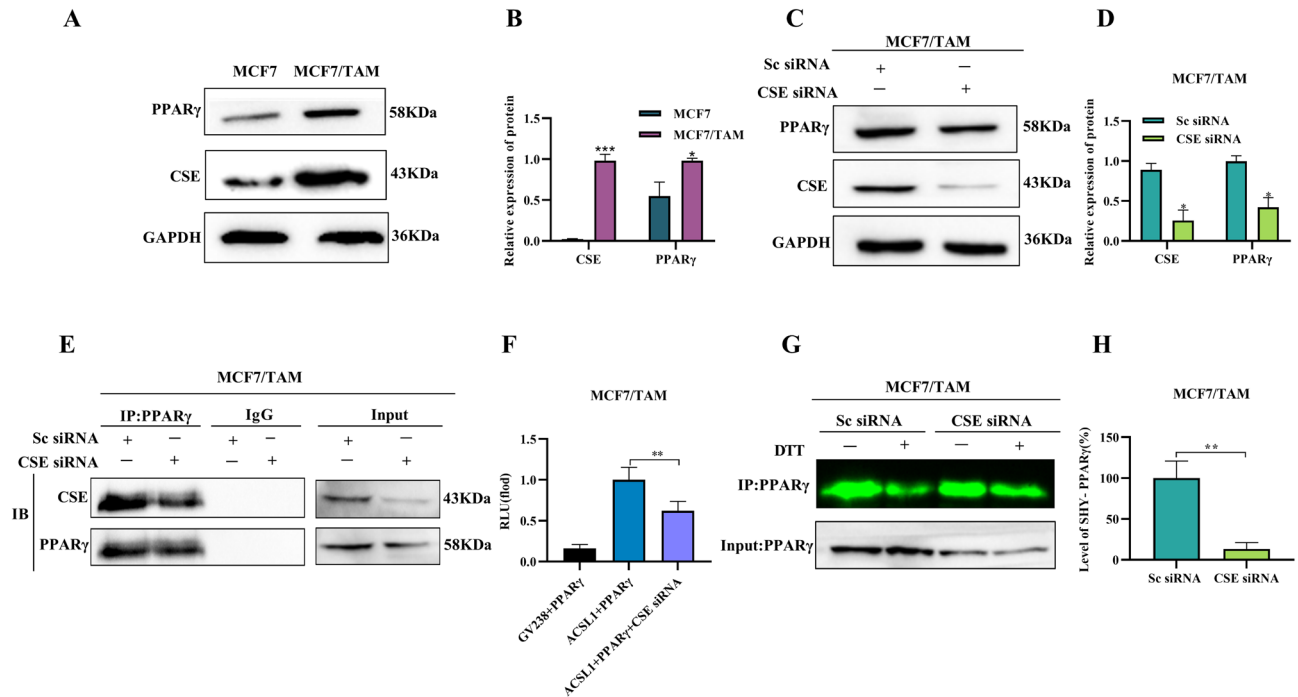


**Fig. 6.** ACSL1 expression in MCF7/TAM cells is regulated by CSE through protein interactions and sulfhydrylation modification of PPAR $\gamma$ . (A and B) Expression levels of PPAR $\gamma$  in ER+ breast cancer TAM-resistant cells MCF7/TAM. All data are expressed as mean  $\pm$  standard deviation (n = 3). \* $P$  < 0.05, \*\*\* $P$  < 0.001 versus MCF7 cells. (C and D) Effect of down-regulation of CSE on PPAR $\gamma$  expression in MCF7/TAM cells. All data are expressed as mean  $\pm$  standard deviation (n = 3). \* $P$  < 0.05 versus Sc siRNA group. (E) CSE interaction with PPAR $\gamma$ . The overexpression plasmids of CSE and PPAR $\gamma$  were cotransfected into MCF7/TAM cells, followed by co-immunoprecipitation assay. (F) Effect of down-regulation of CSE on PPAR $\gamma$  binding to the ACSL1 promoter in MCF7/TAM cells. Overexpression plasmids of ACSL1 promoter and PPAR $\gamma$  were cotransfected into MCF7/TAM cells, which were then assayed by applying a dual luciferase reporter gene assay kit. All data are expressed as mean  $\pm$  standard deviation (n = 3). \*\* $P$  < 0.01 versus ACSL1 + PPAR $\gamma$  group. (G and H) Effect of down-regulation of CSE protein on PPAR $\gamma$  sulfhydrylation levels in MCF7/TAM cells. The maleimide method was applied to detect the level of PPAR $\gamma$  sulfhydrylation. All data are expressed as mean  $\pm$  standard deviation (n = 3). \*\* $P$  < 0.01 versus Sc siRNA group.

which CSE influences cellular signalling pathways, as well as the potential implications for human health. This information may have important ramifications for future research and development efforts in the field.

Further research is required to investigate the impact of CSE inhibitors on reducing drug resistance and to determine whether CSE may be used as a biomarker of TAM resistance. We discovered that I194496, a new CSE inhibitor, increased the susceptibility of TAM-resistant breast cancer cells to TAM treatment and overcame resistance through the PPAR $\gamma$ /ACSL1/STAT3 pathway. In the next study, we will perform experiments using different TAM-resistant ER-positive BC cell lines to validate the broad effect and specificity of I194496. And to delve into its mechanism of action, such as delving into how precisely I194496 regulates the STAT3 pathway, including what the direct targets are and how this interaction affects downstream signaling. And extend the study to the downstream effects of STAT3, such as the correlation with biological processes (cell cycle, apoptosis and autophagy etc.). These studies are important for understanding and overcoming pharmacological resistance in ER-positive BC, especially the therapeutic potential associated with STAT3 inhibition. On this basis, the long-term effects, safety, and possible side effects of I194496 will be further explored.

In summary, CSE could serve as a biomarker of TAM resistance. The new CSE inhibitor I194496 successfully alleviated the TAM-induced reduction in resistance in ER-positive breast cancer cells by activating PPAR $\gamma$ . This modulates the expression of ACSL1 and affects the activation of STAT3 (Fig. 10).

## Methods

### Cell lines

The Key Laboratory of Natural Medicine and Immune-Engineering at Henan University (Kaifeng, China) supplied the breast cancer cell line MCF7, and Xiamen University's School of Pharmacy donated T47D. The human normal breast cell line Hs578bst was purchased from Guan DAO Biological Engineering Co., Ltd. (Shanghai, China). The cells were cultured in Dulbecco's modified Eagle's medium (DMEM) (Solarbio, China) and RPMI 1640 medium (Gibco, USA) supplemented with 10% foetal bovine serum (FBS; Zeta Life, USA) at 37 °C in a 5% CO<sub>2</sub> atmosphere. The vendors authenticated the cell lines.



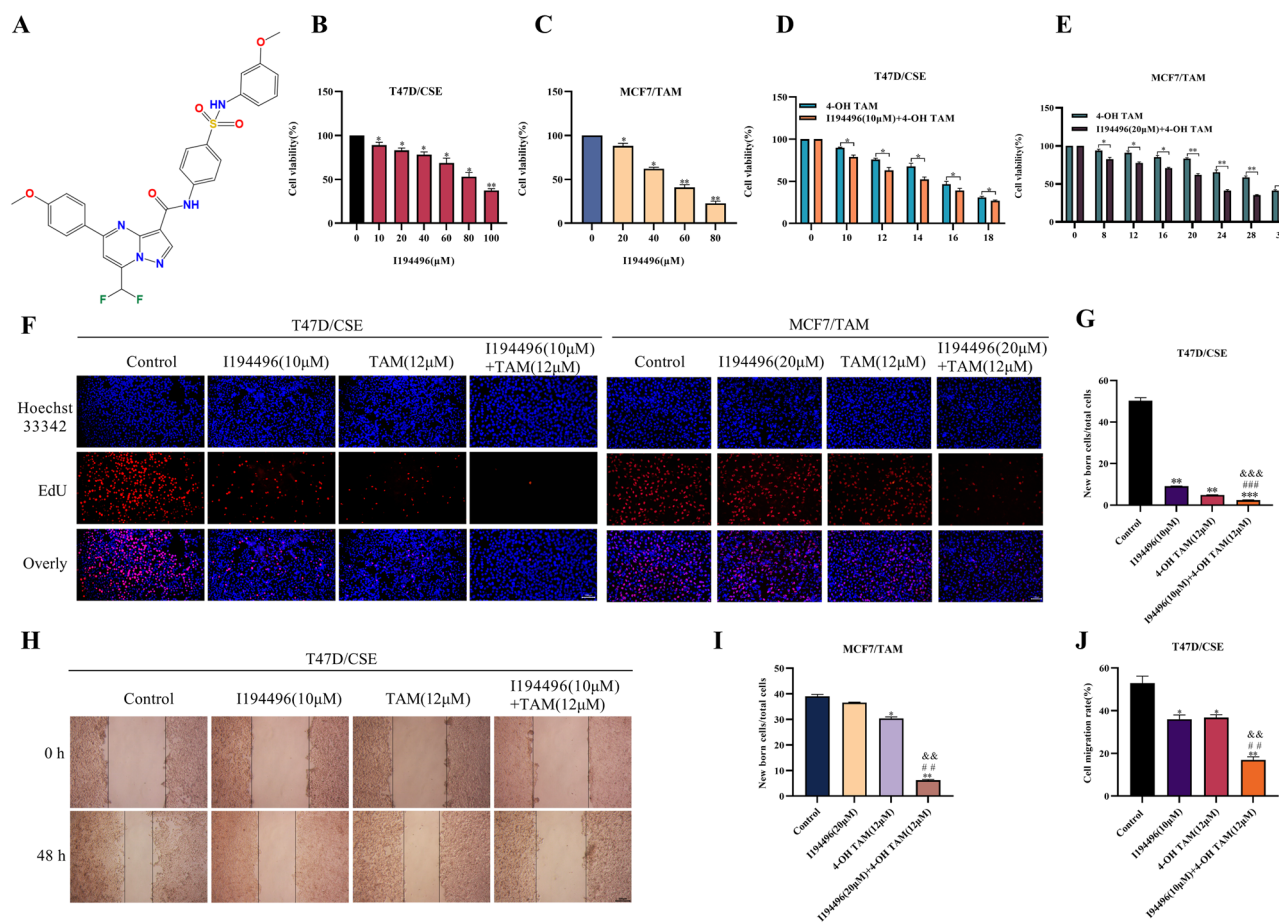


**Fig. 7.** Application of I194496 increased the inhibitory effect of TAM on the growth, proliferation, migration effect of breast cancer cells. **(A)** The chemical structure of the compound I194496. **(B–E)** Effect of applying I194496 on the growth of T47D/CSE and MCF7/TAM cells was detected by MTS assay. All data are expressed as mean  $\pm$  standard deviation (n = 3). \* $P < 0.05$  versus 0  $\mu\text{M}$  I194496 group. **(F,G,I)** Effect of applying I194496 in combination with TAM on the growth and proliferation of T47D/CSE and MCF7/TAM cells was detected by EdU assays. Scale bars, 100  $\mu\text{m}$ . All data are expressed as mean  $\pm$  standard deviation (n = 3). \* $P < 0.05$ , \*\* $P < 0.01$  versus 4-OH TAM group. **(H,J)** Effect of applying I194496 in combination with TAM on the migration of T47D/CSE cells was detected by wound healing assay. Representative images were taken. Scale bars, 500  $\mu\text{m}$ .

## Drug and compound

4-Hydroxy TAM was purchased from MCE Technology (HY16950, China). Compound I194496, a new CSE inhibitor discovered by virtual screening and verified using experimental methods<sup>21,26</sup>, was purchased from Compound Handling B.V. Figure 7A shows the chemical structure of Compound I194496.

## Plasmid construction and lentivirus infection

To create a CSE-knockdown lentivirus, full-length CSE cDNA was cloned and inserted into the hU6-MCS-CbhcGFP-IRES-puromycin vector from Shanghai GeneChem Co., Ltd. The CSE-knockdown lentivirus was applied to infect MCF7 cells, resulting in stable cells with downregulated CSE. In addition, MCF7/TAM cells in six-well plates were transfected with either scramble siRNA (Sc siRNA, 20  $\mu\text{M}$ ), a specific siRNA against human CSE (20  $\mu\text{M}$  Invitrogen; Shanghai GenePharma Co., Ltd.), or a specific siRNA against human ACSL1 (20  $\mu\text{M}$  Invitrogen; Shanghai GenePharma Co., Ltd.) with Lipofectamine 2000<sup>®</sup> (Invitrogen; Thermo Fisher Scientific, Inc.). The siRNA sequences used were as follows: CSE-specific siRNA sense, 5'-GGUUUAGCAGCCACUGUAAdTdT-3' and antisense, 5'-UUACAGUGGCUGCUAAACCCdTdT-3'; ACSL1-specific siRNA sense, 5'-GCGGCAUCAUCA GAAACAATT-3' and antisense, 5'-UUGUUUCUGAUGAUGCCGCTT-3'; and Sc siRNA sense, 5'-UUCUCC GAACGUGUCACGUTT-3' and antisense, 5'-ACGUGACACGUUCGGAGAATT-3'. To overexpress PPAR $\gamma$ , MCF7/TAM cells were transfected with PPAR $\gamma$  overexpression plasmids (pcDNA 3.1(+)-vector and pcDNA 3.1(+)-PPAR $\gamma$ , Nanjing Tsingke Biotech Co., Ltd.) or ACSL1 promoter overexpression plasmids (GV238-vector and GV238-ACSL1, Shanghai GeneChem Co., Ltd.).

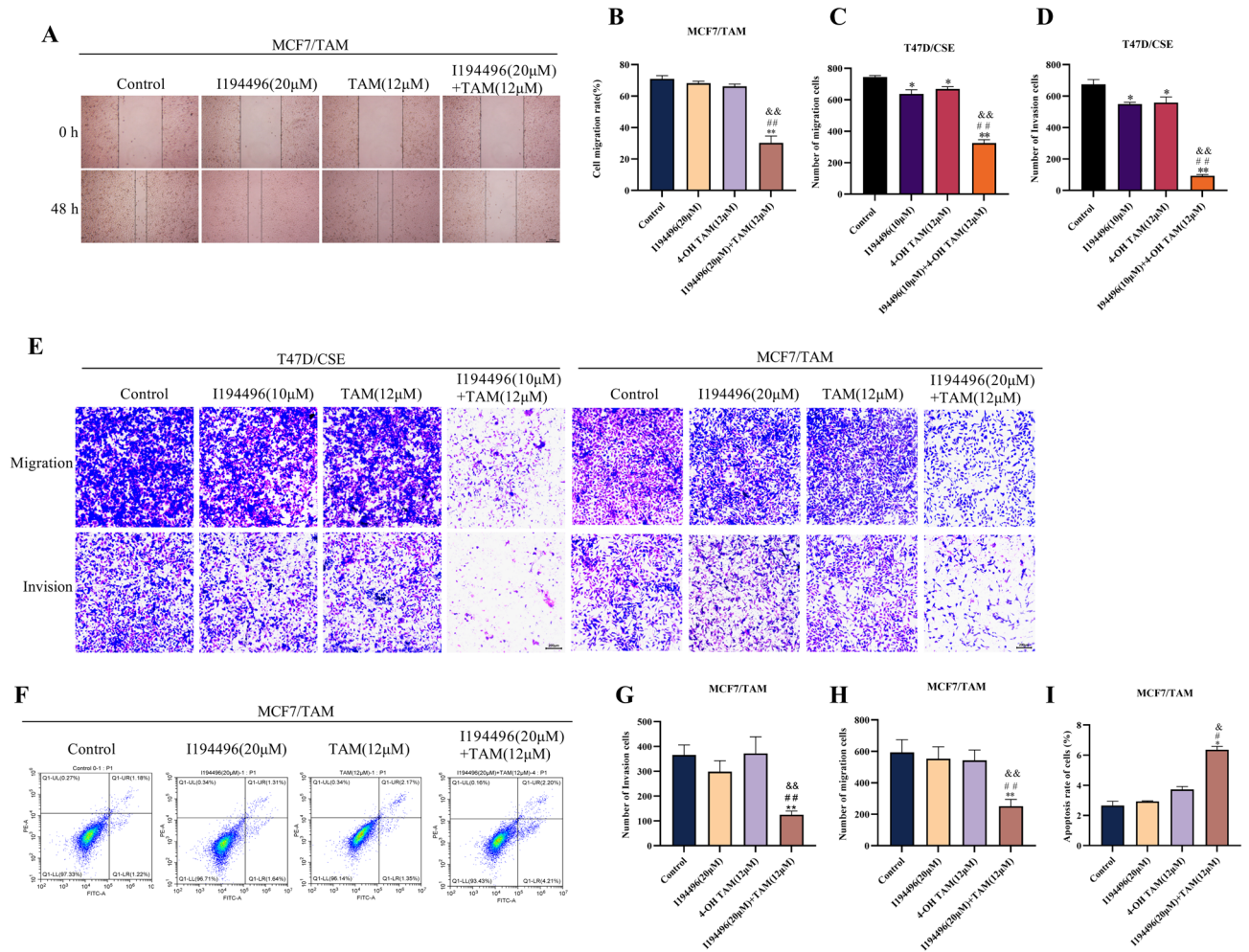


**Fig. 8.** Application of I194496 increased the inhibitory effect of TAM on the migration, invasion and the apoptosis-promoting effect of breast cancer cells. (A–B) Effect of applying I194496 in combination with TAM on the migration of MCF7/TAM cells was detected by wound healing assay. Representative images were taken. Scale bars, 500 μm. (C–E, G, H) Effect of applying I194496 in combination with TAM on the migration and invasion of T47D/CSE and MCF7/TAM cells was performed by transwell assay. cells. Representative images were taken. Scale bars, 200 μm. (F and I) Effect of applying I194496 in combination with TAM on the apoptosis of MCF7/TAM cells was performed by apoptosis assay. cell. All data are expressed as mean ± standard deviation (n = 3). \**P* < 0.05, \*\**P* < 0.01 versus Control group. #*P* < 0.05, ##*P* < 0.01 versus I194496 group. &*P* < 0.05, &&*P* < 0.01 versus 4-OH TAM (12 μM) group.

### Establishment of TAM-resistant cells

MCF7 cells were grown in DMEM supplemented with 4-hydroxy TAM at concentrations ranging from 1 to 5 μM for over 8 months to establish TAM-resistant MCF7/TAM breast cancer cells. The cells were then cultured in DMEM supplemented with 1 μM TAM.

### MTS and EdU assays

Cell viability was determined using an MTS kit (Sigma, M8180). Cells were seeded in 96-well plates at a density of  $1 \times 10^4$  cells per well for 24 h. The cells were subsequently treated with various doses of 4-hydroxy TAM or I194496 for 48 h. MTS was applied to the cells for 4 h, and the OD value was determined at 570 nm using a microplate spectrophotometer. EdU assays were used to measure cell proliferation. Cells were treated with 4-hydroxy TAM or I194496 for 48 h, and proliferating cells were detected using an EdU test kit (Guangzhou RiboBio Co., Ltd., China). In brief, the procedure involved EdU labelling, cell fixation, Apollo staining, and DNA staining. Each experiment was carried out in triplicate.

### Scratch assay

A total of  $8 \times 10^5$  cells were seeded in 6-well plates. When the cells reached 90% confluence, they were scraped with a 200 μl pipette tip on 35 mm dishes. TAM was then added at various concentrations. After a 48-h incubation period, migratory images were taken at 0 and 48 h after scraping to compare the gap closure rates.

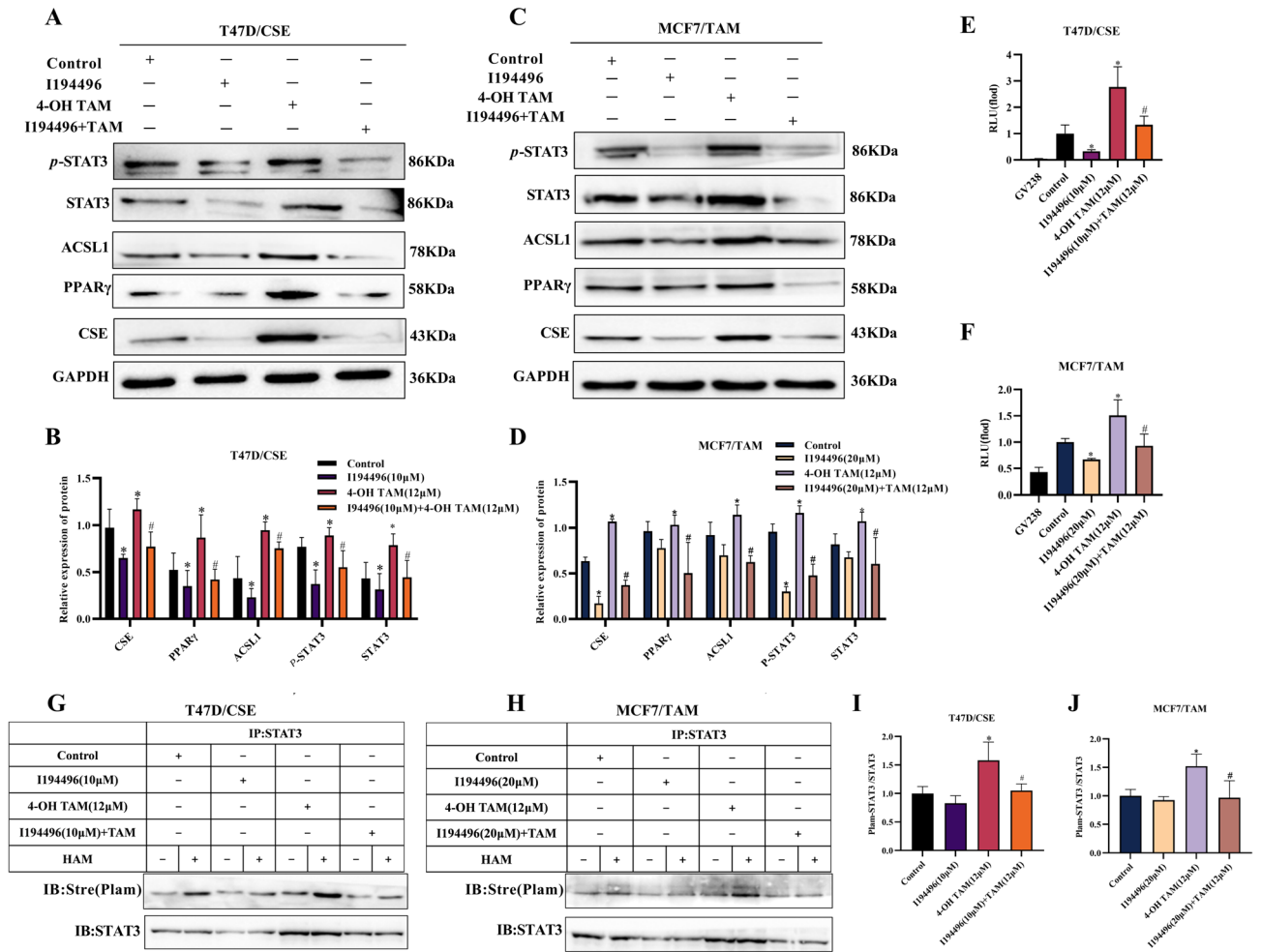


**Fig. 9.** I194496 can reverse CSE-regulated PPAR $\gamma$ /ACSL1/STAT3 pathway signaling in T47D/CSE and MCF7/TAM of breast cancer cells. (A–D) Effect of I194496 in combination with TAM on PPAR $\gamma$ , ACSL1, STAT3, p-STAT3, and CSE protein expression in T47D/CSE and MCF7/TAM cells. (E and F) Effect of I194496 in combination with TAM on PPAR $\gamma$  binding activity to the ACSL1 promoter in T47D/CSE and MCF7/TAM cells. The overexpression plasmids of ACSL1 promoter and PPAR $\gamma$  were cotransfected into T47D/CSE and MCF7/TAM cells, and then assayed by applying a dual luciferase reporter gene assay kit. (G–J) Effect of I194496 in combination with TAM on STAT3 palmitoylation in T47D/CSE and MCF7/TAM cells. The acyl-biotin substitution method was applied to detect STAT3 palmitoylation. All data are expressed as mean  $\pm$  standard deviation (n = 3). \*P < 0.05 versus Control group. #P < 0.05 versus 4-OH TAM (12  $\mu$ M) group.

### Transwell assay

Cell migration and invasion were tested using a Transwell assay in 24-well chambers (8  $\mu$ m pore size; Corning Incorporated, Corning, NY, USA). The Transwell chambers were covered with or without Matrigel matrix (BD Biosciences, CA, USA) for invasion and migration assays. The specific procedure is described in references<sup>26,30,31</sup>. In the upper chamber,  $8 \times 10^5$  cells were added to serum-free media. In the lower chamber, medium containing 10% FBS was added. After 48 h of incubation, the cells were fixed and stained. Photos were taken after drying. The number of cells indirectly represented the potential of the cells to migrate and invade.

### Western blot analysis

The cells were washed with ice-cold phosphate-buffered saline (PBS) before being lysed on ice for 20 min in RIPA lysis buffer (ProteinTech Group, Inc.) containing protease and phosphatase inhibitors. Protein concentrations were measured using a BCA protein assay kit (Solarbio, China), and Western blot analysis was carried out following a predetermined protocol. The primary and secondary antibodies used were CSE antibody (1:3000, cat. no. CY8267, Abways Technology), ACSL1 antibody (1:3000, cat. no. 13989-1-AP, ProteinTech Group, Inc.), PPAR $\gamma$  antibody (1:3000, cat. no. 16643-1-AP, ProteinTech Group, Inc.), STAT3 antibody (1:3000, cat. no. 51076-2-AP, ProteinTech Group, Inc.), p-STAT3 antibody (1:3000, cat. no. CY6566, Abways Technology), GAPDH antibody (1:100,000, cat. no. 60004-1-Ig, ProteinTech Group, Inc.), HRP-goat anti-rabbit IgG (1:3000, cat. no. SA00001-2, ProteinTech Group, Inc.), HRP-goat anti-mouse IgG (1:3000, cat. no. SA00001-1, ProteinTech Group, Inc.), and HRP-streptavidin (1:200, cat. no. A0303, Beyotime, China).

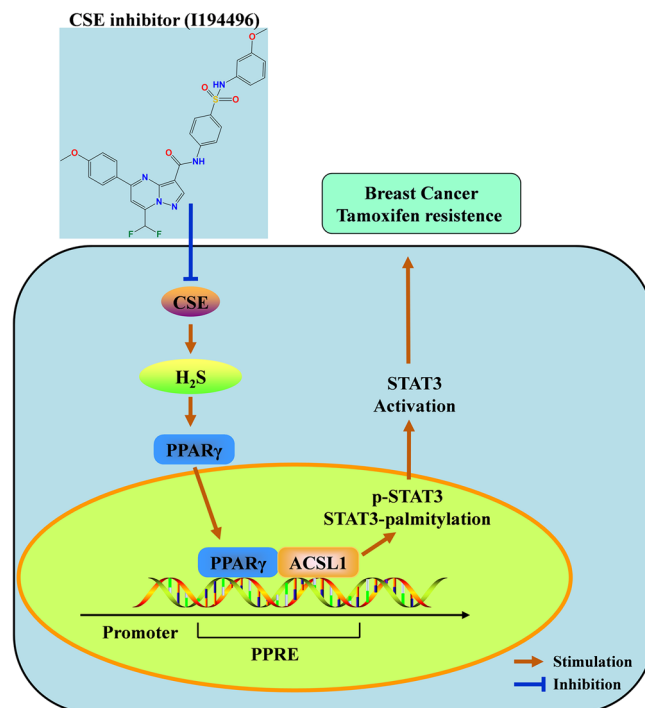


**Fig. 10.** Schematic diagram of the regulation of CSE and its inhibitor I194496 on TAM resistant breast cancer cells.

### Determination of H<sub>2</sub>S production

The methylene blue method was used to determine H<sub>2</sub>S<sup>32</sup>. Cells in the logarithmic growth phase were collected by centrifugation and resuspended in 1 ml of culture media before being injected into six-well plates after counting. On the second day after cell walling, 40  $\mu$ l of L-cysteine (2 mmol/L), 100  $\mu$ l of pyridoxal 5-phosphate (0.5 mmol/l), and serum-free media containing the corresponding concentration of TAM were added to each well. The final volume of liquid in each well was 2 ml. Moreover, 500  $\mu$ l of 1% (w/v) zinc acetate was applied dropwise to the filter paper. After 48 h, the filter paper was removed from the plates and placed in 15 ml centrifuge tubes. Then, 500  $\mu$ l of 0.2% (w/v) N,N-dimethyl-p-phenylenediamine dihydrochloride dye, 50  $\mu$ l of 10% (w/v) ferric ammonium sulfate, and 3 ml of deionized water were added to the centrifuge tubes, mixed gently, and then incubated in a 37 °C oven for 20 min. After a sufficient reaction, the supernatant was centrifuged and transferred to a 96-well plate (200  $\mu$ l per well). Using a multifunctional enzyme marker, the absorbance was measured at 670 nm. A standard curve was used to determine the H<sub>2</sub>S concentration, and the release was expressed as nmol·min<sup>-1</sup> per 1  $\times$  10<sup>6</sup> cells.

### Coimmunoprecipitation

The cells were lysed using NP-40 lysis buffer (Solarbio, China), and the lysates were then treated with protein A + G agarose (cat. no. P2055, Beyotime, China) and a PPAR<sub>γ</sub> antibody conjugated overnight at 4 °C. Three washes of the beads containing affinity-bound proteins were performed using PBS buffer. This was followed by three elutions using NP-40 lysis buffer. Protein samples were separated on sodium dodecyl sulfate polyacrylamide gels, denatured, and then transferred to polyvinylidene fluoride membranes using 40  $\mu$ l of 2  $\times$  loading buffer. Next, the membrane was detected and probed using the designated antibodies.

### Dual-luciferase reporter assay

The dual-luciferase reporter assay method was used according to Guo et al.<sup>33</sup>. To assess the effect of the down-regulation of CSE expression on the binding of the ACSL1 promoter to PPAR<sub>γ</sub>, four tubes were divided into two groups. In group one, 800 ng of PPAR<sub>γ</sub> overexpression plasmid, 800 ng of GV238-ACSL1-luciferase promoter plasmid, and 40 ng of pRL-TK plasmid were added to one EP tube with a luciferase:sea kidney ratio of 30:1. The identical plasmid indicated above was injected into another tube, along with 1  $\mu$ l of CSE siRNA. In group two, 2.4  $\mu$ l of Lipofectamine 2000 was added to two EP tubes. Each tube was mixed gently and incubated at room temperature for 5 min. Then, the tubes of groups one and two were mixed and incubated for 20 min. To assess the effect of the CSE inhibitor I194496 on the binding of the ACSL1 promoter to PPAR<sub>γ</sub>, nontoxic doses of I194496, TAM, and the combination of the two were introduced to the same group two as above. After lysis, washing and transfection, the luciferase activities were assessed for 48 h using a dual-luciferase reporter kit (Yeasen Biotechnology, Shanghai, China). Every experiment was conducted three times.

### ABE analysis

The palmitoylation of proteins was established by using the ABE method<sup>34</sup>. In brief, NP40 lysis buffer containing 50 mM NEM was added to ice for lysis. Overnight immunoprecipitation of the samples was performed using a STAT3 antibody. The next day, 40  $\mu$ L of protein A + G agarose beads was added, and the mixture was shaken for 4 h at 4 °C. After the precipitate was blocked in lysis buffer containing 10 mM NEM, stringent buffer (lysis buffer, 10 mM NEM, and 0.1% SDS) and lysis buffer were used for washing. The sample was split into two equal parts: one was treated with 1 M hydroxylamine (HAM) for 50 min at room temperature to disrupt thioester linkages, and the other (HAM-) was used as a control. The bead precipitate was mixed with 500  $\mu$ L of 2  $\mu$ M biotin-HPDP buffer, and the mixture was shaken for 50 min at 4 °C. The reaction mixture was then washed once with lysis buffer (pH 6.2) and 3 times with lysis buffer. After the addition of loading buffer, the precipitate was heated in a protein cooker. Streptavidin–horseradish peroxidase (Beyotime, China) was utilized to identify the proteins following electrophoresis and membrane transfer.

### Maleimide method

We used a maleimide assay to detect PPAR $\gamma$  sulfhydrylation. The method of Paul et al. was modified<sup>35</sup>. Briefly, the cells were lysed with NP40 lysis buffer. PPAR $\gamma$  antibody was used to immunoprecipitate the samples overnight. The next day, 40  $\mu$ L of protein A + G agarose beads and fluorescein-5-maleimide (final concentration 2  $\mu$ M) were added to all EP tubes and incubated for 4 h in the dark in a 4 °C refrigerator with shaking. After washing, the samples were divided into two portions. One set was treated with 1 mM DTT. All samples were rotated at 4 °C for 1 h. Western blotting was used to evaluate the proteins after they had been washed three times with lysis buffer.

### Statistical analysis

The data were analysed statistically using GraphPad Prism 8, SPSS 19.0, and ImageJ software, and the data are expressed as the mean and standard deviation. One-way ANOVA was used to assess differences between experimental groups with a single variable, and two-way ANOVA was used to determine the statistical significance of differences between experimental groups with two variables, followed by Tukey's multiple comparisons test (Supplementary Figure 1).

### Data availability

The data sets analyzed during the current study are available from the corresponding author.

Received: 13 March 2024; Accepted: 2 September 2024

Published online: 03 October 2024

### References

1. Azamjah, N., Soltan Zadeh, Y. & Zayeri, F. Global trend of breast cancer mortality rate: A 25-year study. *Asian Pac. J. Cancer Prev.* **20**(7), 2015–2020 (2019).
2. Miller, K. D. et al. Cancer treatment and survivorship statistics. *CA Cancer J. Clin.* **72**(5), 409–436 (2022).
3. Giovannelli, P. et al. The androgen receptor in breast cancer. *Front. Endocrinol. (Lausanne)*. **9**, 492 (2018).
4. Mohammed, A. A. The clinical behavior of different molecular subtypes of breast cancer. *Cancer Treat. Res. Commun.* **29**, 100469 (2021).
5. Hanker, A. B., Sudhan, D. R. & Arteaga, C. L. Overcoming endocrine resistance in breast cancer. *Cancer Cell.* **37**(4), 496–513 (2020).
6. Donnarumma, E., Trivedi, R. K. & Lefer, D. J. Protective actions of H<sub>2</sub>S in acute myocardial infarction and heart failure. *Compr. Physiol.* **7**(2), 583–602 (2017).
7. Hellmich, M. R., Coletta, C., Chao, C. & Szabo, C. The therapeutic potential of cystathionine beta-synthetase/hydrogen sulfide inhibition in cancer. *Antioxid. Redox Signal.* **22**(5), 424–448 (2015).
8. Dong, Q. et al. A novel hydrogen sulfide-releasing donor, HA-ADT, suppresses the growth of human breast cancer cells through inhibiting the PI3K/AKT/mTOR and Ras/Raf/MEK/ERK signaling pathways. *Cancer Lett.* **455**, 60–72 (2019).
9. Khattak, S. et al. Hydrogen sulfide biology and its role in cancer. *Molecules.* **27**(11), 3389 (2022).
10. Wang, M., Yan, J., Cao, X., Hua, P. & Li, Z. Hydrogen sulfide modulates epithelial-mesenchymal transition and angiogenesis in non-small cell lung cancer via HIF-1 $\alpha$  activation. *Biochem. Pharmacol.* **172**, 113775 (2020).
11. Yang, Y. L. et al. The role of hydrogen sulfide in the development and progression of lung cancer. *Molecules.* **27**(24), 9005 (2022).
12. Zheng, H. et al. Nifuratel, a novel STAT3 inhibitor with potent activity against human gastric cancer cells. *Cancer Manag. Res.* **9**, 565–572 (2017).
13. Kolosenko, I. et al. Identification of novel small molecules that inhibit STAT3-dependent transcription and function. *PLoS One.* **12**(6), e0178844 (2017).
14. Zhu, N. et al. Loss of ZIP facilitates JAK2-STAT3 activation in tamoxifen-resistant breast cancer. *Proc. Natl. Acad. Sci. U S A.* **117**(26), 15047–15054 (2020).
15. Bui, Q. T. et al. Essential role of Notch4/STAT3 signaling in epithelial-mesenchymal transition of tamoxifen-resistant human breast cancer. *Cancer Lett.* **390**, 115–125 (2017).
16. Tsoi, H., Man, E. P. S., Chau, K. M. & Khoo, U. S. Targeting the IL-6/STAT3 signalling cascade to reverse tamoxifen resistance in Estrogen receptor positive breast cancer. *Cancers (Basel)*. **13**(7), 1511 (2021).
17. Xu, Y. et al. Tamoxifen attenuates reactive astrocyte-induced brain metastasis and drug resistance through the IL-6/STAT3 signaling pathway. *Acta Biochim. Biophys. Sin. (Shanghai)*. **52**(12), 1299–1305 (2020).
18. You, J. et al. Cystathionine- $\gamma$ -lyase promotes process of breast cancer in association with STAT3 signaling pathway. *Oncotarget.* **8**(39), 65677–65686 (2017).
19. Liu, Y. et al. A novel cystathionine  $\gamma$ -lyase inhibitor, I194496, inhibits the growth and metastasis of human TNBC via down-regulating multiple signaling pathways. *Sci. Rep.* **11**(1), 8963 (2021).
20. Wang, Y. et al. HBXIP up-regulates ACSL1 through activating transcriptional factor Sp1 in breast cancer. *Biochem. Biophys. Res. Commun.* **484**(3), 565–571 (2017).
21. Niu, J. et al. Fatty acids and cancer-amplified ZDHHC19 promote STAT3 activation through S-palmitoylation. *Nature.* **573**(7772), 139–143 (2019).

22. Li, T., Li, X., Meng, H., Chen, L. & Meng, F. ACSL1 affects triglyceride levels through the PPARgamma pathway. *Int. J. Med. Sci.* **17**(6), 720–727 (2020).
23. Leonardini, A. *et al.* Cross-talk between PPAR $\gamma$  and insulin signaling and modulation of insulin sensitivity. *PPAR. Res.* **2009**, 818945 (2009).
24. Paul, B. D. & Snyder, S. H. H<sub>2</sub>S: A novel gasotransmitter that signals by sulfhydration. *Trends Biochem. Sci.* **40**(11), 687–700 (2015).
25. Davies, C. *et al.* Long-term effects of continuing adjuvant tamoxifen to 10 years versus stopping at 5 years after diagnosis of oestrogen receptor-positive breast cancer: ATLAS, a randomised trial. *Lancet.* **381**(9869), 805–816 (2013).
26. Wang, L. *et al.* I157172, a novel inhibitor of cystathionine gamma-lyase, inhibits growth and migration of breast cancer cells via SIRT1-mediated deacetylation of STAT3. *Oncol. Rep.* **41**(1), 427–436 (2019).
27. Goetz, M. P. *et al.* Pharmacogenetics of tamoxifen biotransformation is associated with clinical outcomes of efficacy and hot flashes. *J. Clin. Oncol.* **23**(36), 9312–9318 (2005).
28. Silver, D. J. *et al.* Severe consequences of a high-lipid diet include hydrogen sulfide dysfunction and enhanced aggression in glioblastoma. *J. Clin. Invest.* **131**(17), e138276 (2021).
29. Rohrig, F. & Schulze, A. The multifaceted roles of fatty acid synthesis in cancer. *Nat. Rev. Cancer.* **16**(11), 732–749 (2016).
30. Wang, L. *et al.* Cystathionine-gamma-lyase promotes the metastasis of breast cancer via the VEGF signaling pathway. *Int. J. Oncol.* **55**(2), 473–487 (2019).
31. Nitti, M. *et al.* HO-1 induction in cancer progression: A matter of cell adaptation. *Antioxidants (Basel).* **6**(2), 29 (2017).
32. Wang, L. *et al.* Cystathionine- $\gamma$ -lyase promotes the metastasis of breast cancer via the VEGF signaling pathway. *Int. J. Oncol.* **55**, 473–487 (2019).
33. Guo, L. *et al.* The function of SNHG7/miR-449a/ACSL1 axis in thyroid cancer. *J. Cell. Biochem.* **121**(10), 4034–4042 (2020).
34. Brigidi, G. S. & Bamji, S. X. Detection of protein palmitoylation in cultured hippocampal neurons by immunoprecipitation and acyl-biotin exchange (ABE). *J. Vis. Exp.* **72**, 50031 (2013).
35. Paul, B. D. & Snyder, S. H. Protein sulfhydration. *Methods Enzymol.* **555**, 79–90 (2015).

## Acknowledgements

This work was supported by National Natural Science Foundation of China (No. 82072726); The Natural Science Foundation of Henan Province in China (No. 202300410079).

## Author contributions

L.K.J., L.M. and W.T.X. acquired funding, conceived and designed the experiments. F.H. and H.X. performed the review and experiments. G.W.Q., Z.X.N., Y.C.X., Z.W., F.S.S., W.J. and Z.Z.S. analyzed the data and produced the figures. L.K.J., F.H. and W.T.X. wrote and revised the manuscript. All authors reviewed the manuscript.

## Competing interest

The authors declare no competing interests.

## Additional information

**Supplementary Information** The online version contains supplementary material available at <https://doi.org/10.1038/s41598-024-71962-7>.

**Correspondence** and requests for materials should be addressed to K.L., M.L. or T.W.

**Reprints and permissions information** is available at [www.nature.com/reprints](http://www.nature.com/reprints).

**Publisher's note** Springer Nature remains neutral with regard to jurisdictional claims in published maps and institutional affiliations.

**Open Access** This article is licensed under a Creative Commons Attribution-NonCommercial-NoDerivatives 4.0 International License, which permits any non-commercial use, sharing, distribution and reproduction in any medium or format, as long as you give appropriate credit to the original author(s) and the source, provide a link to the Creative Commons licence, and indicate if you modified the licensed material. You do not have permission under this licence to share adapted material derived from this article or parts of it. The images or other third party material in this article are included in the article's Creative Commons licence, unless indicated otherwise in a credit line to the material. If material is not included in the article's Creative Commons licence and your intended use is not permitted by statutory regulation or exceeds the permitted use, you will need to obtain permission directly from the copyright holder. To view a copy of this licence, visit <http://creativecommons.org/licenses/by-nc-nd/4.0/>.

© The Author(s) 2024